Journal of Rheology

RESEARCH ARTICLE | MARCH 27 2024

Strain shift measured from stress-controlled oscillatory shear: Evidence for a continuous yielding transition and new techniques to determine recovery rheology measures

James J. Griebler ; Gavin J. Donley ; Victoria Wisniewski; Simon A. Rogers

J. Rheol. 68, 301–315 (2024)
https://doi.org/10.1122/8.0000756

Strain shift measured from stress-controlled oscillatory shear: Evidence for a continuous yielding transition and new techniques to determine recovery rheology measures

James J. Griebler,[1] Gavin J. Donley,[2] Victoria Wisniewski,[1] and Simon A. Rogers[1,a)]

[1]*Chemical and Biomolecular Engineering Department, The University of Illinois Urbana-Champaign, Urbana, Illinois 61801*
[2]*Physics Department, Georgetown University, Washington, DC 20057*

(Received 30 August 2023; final revision received 30 January 2024; published 27 March 2024)

Abstract

Understanding the yielding of complex fluids is an important rheological challenge that affects our ability to engineer and process materials for a wide variety of applications. Common theoretical understandings of yield stress fluids follow the Oldroyd–Prager formalism in which the material behavior below the yield stress is treated as solidlike, and above the yield stress as liquidlike, with an instantaneous transition between the two states. This formalism was built on a quasi-static approach to the yield stress, while most applications, ranging from material processing to end user applications, involve a transient approach to yielding over a finite timescale. Using stress-controlled oscillatory shear experiments, we show that yield stress fluids flow below their yield stresses. This is quantified through measuring the strain shift, which is the value about which the strain oscillates during a stress-controlled test and is a function of only the unrecoverable strain. Measurements of the strain shift are, therefore, measurements of flow having taken place. These experimental results are compared to the Herschel–Bulkley form of the Saramito model, which utilizes the Oldroyd–Prager formalism, and the recently published Kamani–Donley–Rogers (KDR) model, in which one constitutive equation represents the entire range of material responses. Scaling relationships are derived, which allow us to show why yield stress fluids will flow across all stresses, above and below their yield stress. Finally, derivations are presented that show strain shift can be used to determine average metrics previously attainable only through recovery rheology, and these are experimentally verified. https://doi.org/10.1122/8.0000756

I. INTRODUCTION

Yield stress fluids are ubiquitous in many industries ranging from foods and cosmetics to additive manufacturing, building materials, biomedical research, and more [1–6]. These materials are desirable for their ability to flow under processing conditions and then hold their shape when external forces are removed. Recently, natural phenomena such as avalanches and mudslides have also been shown to exhibit yielding behaviors, which makes the understanding of yielding applicable to industrial, environmental, humanitarian, and economic interest, as the yielding transition is the difference between a stable hillside and a catastrophic disaster [7–9].

The distinction between material behaviors was first discussed in the work of Oldroyd, where a yield stress fluid was described as having two different constitutive responses, one each above and below the yield stress. These two material states were separated by a binary transition between the two responses. Along with early works by Prager, this distinction of two constitutive responses, separated by the yield stress has become to be known as the Oldroyd–Prager formalism [10–12]. When Oldroyd introduced this idea, he explicitly considered only a quasi-static approach to the yield stress [10], meaning that this approach should only be applied in the limit of infinitely long times or infinitely low frequencies. However, the quasi-static stipulation is often ignored, and it is commonly assumed that no flow occurs below the yield stress under transient conditions [13–16].

A. Introduction to recovery rheology through common mechanical models

To separate what it means to be solidlike and liquidlike, we can look at early rheological works that discuss how the strain a material experiences is made up of recoverable and unrecoverable components. The strain and strain rate are, therefore, composite measures [17,18],

$$\gamma(t) = \gamma_{\text{rec}}(t) + \gamma_{\text{unrec}}(t), \tag{1}$$

$$\dot{\gamma}(t) = \dot{\gamma}_{\text{rec}}(t) + \dot{\gamma}_{\text{unrec}}(t). \tag{2}$$

Here, γ, γ_{rec}, and γ_{unrec} are the total, recoverable, and unrecoverable strains, and $\dot{\gamma}$, $\dot{\gamma}_{\text{rec}}$, and $\dot{\gamma}_{\text{unrec}}$ are the rates at which strain is acquired in each of the three manners.

An idealized model for an elastic solid response is a Hookean spring as shown in Fig. 1(a). In this simple model, the stress is linearly proportional to the strain, all of which is acquired recoverably, through a modulus

$$\sigma(t) = G\gamma_{\text{rec}}(t). \tag{3}$$

a)Author to whom correspondence should be addressed; electronic mail: sarogers@illinois.edu

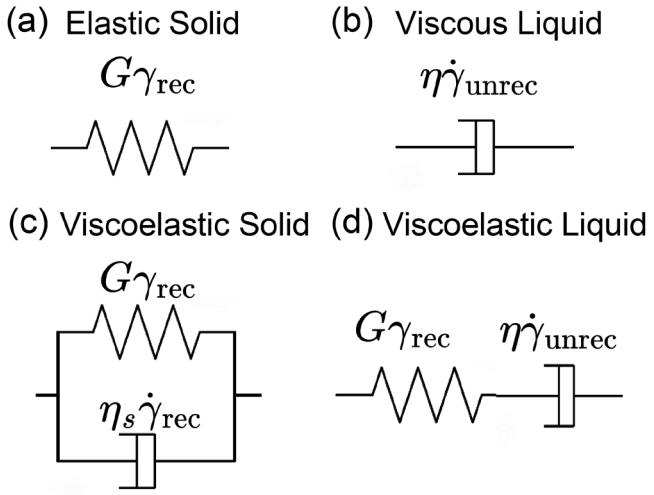

FIG. 1. Common mechanical models in rheology, with the individual elements labeled with the stress in each term. (a) Ideal Hookean elastic spring, (b) ideal Newtonian viscous dashpot, (c) Kelvin–Voigt viscoelastic solid, and (d) Maxwell viscoelastic fluid.

Here, σ is the stress and G is the modulus. When deformed, this simple model will store all energy elastically. When the stress is removed, the spring immediately returns to its starting position. That is, it recovers all the strain that had been acquired.

In contrast, an idealized model for a viscous liquid is a Newtonian fluid, in which the stress is equal to the product of the unrecoverable strain rate and a viscosity, η,

$$\sigma(t) = \eta\dot{\gamma}_{\mathrm{unrec}}(t). \tag{4}$$

When deformed, this simple model will dissipate all energy and none will be stored. Because of the complete lack of storage of energy in this model, when the stress is removed from an idealized viscous fluid, the material remains stationary, and no recovery is observed. Viscous fluids are typically represented by a dashpot, as shown in Fig. 1(b).

There are two common models that can be constructed by combining a single spring and a single dashpot. When a Hookean spring is put in series with a Newtonian dashpot, we obtain the Maxwell viscoelastic liquid, which can be said to represent materials that flow, a mechanical model of which can be seen in Fig. 1(d). In this case, the strains and strain rates in the system are additive, and the stress is the same across each element. The response of the model can be calculated from

$$\dot{\sigma}(t) + \frac{G}{\eta}\sigma(t) = \eta\dot{\gamma}(t), \tag{5}$$

where $\dot{\sigma}$ is the stress rate. The behavior of the Maxwell viscoelastic liquid is such that when the stress is removed, some strain will be recovered by the spring, and some will remain unrecoverable due to the viscous dashpot. During deformation, energy will be stored elastically by the spring while the dashpot will dissipate energy. We, therefore, say that the energy dissipated during deformation was dissipated by unrecoverable processes. Furthermore, the ability of this model to acquire strain unrecoverably indicates that it describes flow.

While the Maxwell model combines a spring and a dashpot in series to create a viscoelastic liquid, combining the same two elements in parallel creates a viscoelastic solid that does not flow. This configuration, shown in Fig. 1(c), is referred to as the Kelvin–Voigt model. In this case, the strain and strain rate across each element are the same and the stress is split across the two. We can calculate the response of this model by solving

$$\sigma(t) = \eta_s\dot{\gamma}_{\mathrm{rec}}(t) + G\gamma_{\mathrm{rec}}(t), \tag{6}$$

where η_s is the viscosity of the dashpot. In this case, all strain acquired by the system under an arbitrary stress is recoverable and the model is said to describe a nonflowing viscoelastic solid. Despite all strain being recoverable, this model will still dissipate energy through the dashpot when deformed. To distinguish between energy dissipated in a Maxwellian viscoelastic liquidlike manner and a Kelvin–Voigt viscoelastic solidlike manner, we, therefore, refer to energy dissipation as being associated with recoverable or unrecoverable processes.

Both the Maxwell and the Kelvin–Voigt models dissipate energy, though one represents a viscoelastic fluid and the other a viscoelastic solid. Energy dissipation is, therefore, insufficient as a discriminator for yielding. Furthermore, dissipation of energy does not imply flow. The major difference between the two models is the way in which strain is acquired. The Kelvin–Voigt viscoelastic solid acquires all strain recoverably, therefore, does not flow, while the Maxwell viscoelastic fluid acquires some strain unrecoverably, and flows. This realization indicates the value of performing recovery tests in identifying flow and yielding transition.

Recovery tests are commonly associated with the second part of a creep and recovery test. In this test protocol, constant stress is applied for a specific duration, followed by the removal of the stress. This recovery step can be implemented at any point in any rheological protocol, as long as the rheometer is capable of applying zero shear stress. By performing a recovery step, information regarding recoverable and unrecoverable strains and their rates of acquisition can be ascertained from any rheological protocol, enhancing our understanding of many materials. In addition, a recovery step can be performed iteratively during the protocol, to determine the transient acquisition of recoverable and unrecoverable strains. This way of thinking about rheological experimentation in a general sense has come to be called "recovery rheology" and provides more information than the conventional rheometry approaches alone. This recovery rheology framework also allows for further understanding that has led to new developments in the experimental and theoretical descriptions of yield stress fluids [19–21].

B. Determination of the yield stress

The most common experimental goal for characterizing yield stress fluids is the determination of yield stress. As

summarized by Dinkgreve *et al.*, there remains a lack of consensus on the best method to determine yield stress [22]. Techniques to determine yield stress come in two classes: those that are in accordance with the quasi-static case assumed by Oldroyd, such as steady shear flow curves, and long-time creep experiments, and those with a timescale associated with them, such as amplitude sweeps or steady shear startup experiments. Some of the methods discussed by Dinkgreve *et al.* include fitting of steady shear experiments, oscillatory amplitude sweeps, and creep experiments.

For the case of steady-state flow curves, experimenters first apply a shear rate until the shear stress response reaches the steady state. The shear rate is then changed stepwise, marking the steady-state shear stress at each step. Once sufficiently low shear rates are achieved, the experiment concludes, and one extrapolates the curve to zero-rate using an empirical fitting equation, such as those put forward by Bingham, Herschel and Bulkley, or Casson [23–25]. This method closely matches the situation explicitly assumed by Oldroyd with a quasi-static approach to yield stress, which may explain why the steady-shear flow curve consistently provides the smallest numerical value of yield stress out of the proposed experimental techniques. As Dinkgreve *et al.* point out, the limitations of this procedure are related to the ability of a given rheometer to apply low enough shear rates and of the time required to achieve steady-state at the smallest shear rates, which is typically a few times the inverse of the shear rate. This is reminiscent of the provocative work by Barnes and Walters when discussing the idea of yield stress as a myth or artifact due to the inability to measure low enough shear rates [26]. The argument of Barnes and Walters is that if low enough rates could be applied for long enough, the materials would flow. The modern interpretation is that yielding occurs over a finite timescale and is an engineering reality [27,28].

Another popular method of determining a yield stress is through an oscillatory amplitude sweep, which involves applying oscillatory shear across a range of stress or strain amplitudes at a fixed frequency. From knowledge of the full transient response of the material, it is possible to determine the storage and loss moduli as functions of the amplitude and frequency. While few works investigate the frequency dependence of the value of yield stress, researchers note that the resulting yield stress determined by any one of a number of metrics is dependent on the chosen frequency of oscillation [29,30].

Many studies of large amplitude oscillatory shearing have led to the generally accepted interpretation that the dynamic moduli are average responses over a period of oscillation. The physical meaning of the dynamic moduli comes from energetic considerations. Briefly, the storage and loss moduli are typically introduced in a geometric manner and are said to relate to the in-phase or out-of-phase components of the resulting stress/strain waveform to the applied strain/stress waveform. This geometric interpretation breaks down in the nonlinear regime, where nonsinusoidal responses can be elicited and a single phase difference cannot be determined. A physical interpretation that is consistent in the linear and nonlinear regions comes from considering energy storage and dissipation mechanisms. In this treatment, we consider elasticity as the only mechanism by which energy is stored and ignore the inertial storage of energy. Storage of energy inertially is likely to be more important at the very largest amplitudes at higher frequencies and is typically neglected in studies of elastoviscoplastic material responses. Using the framework of energy storage and dissipation, the storage and loss modulus are defined as

$$G'(\omega) = \frac{4(W_{\text{stored}}(\omega))_{\text{avg}}}{\gamma_0^2} = \frac{2[\sigma(t)\gamma_{\text{rec}}(t)]_{\text{avg}}}{\gamma_0^2}, \tag{7}$$

$$G''(\omega) = \frac{2(\dot{W}_{\text{diss.}}(\omega))_{\text{avg}}}{\gamma_0^2\omega} = \frac{2[\sigma(t)\dot{\gamma}(t)]_{\text{avg}}}{\omega\gamma_0^2}, \tag{8}$$

where W_{stored} is the elastic energy stored per unit volume and $\dot{W}_{\text{diss.}}$ is the rate of energy dissipation per unit volume [31]. The angular frequency is ω, while $\sigma(t)$, $\gamma_{\text{rec}}(t)$, and $\dot{\gamma}(t)$ are the stress, recoverable strain, and total strain rate waveforms, respectively. γ_0 is the amplitude of the (total) strain waveform. The subscript "avg" represents the average of the function over a period of oscillation. Since each of the energy terms is normalized by the total amplitude, there are recoverable and unrecoverable components contributing to the magnitude of both moduli. Referring to modulus as reflecting either purely elastic or viscous behavior is, therefore, incorrect.

Because the strain and strain rate are made up of two terms, the loss modulus is actually a composite measure of the rate of energy dissipation, which can also be split into two terms. One term accounts for the rate of energy dissipation during acquisition of unrecoverable strains, as seen in Eq. (9), and the other term accounts for energy dissipated during recoverable processes, as seen in Eq. (10),

$$G''_{\text{fluid}}(\omega) = \frac{2(\dot{W}_{\text{diss,fluid}}(\omega))_{\text{avg}}}{\omega\gamma_0^2} = \frac{2[\dot{\gamma}_{\text{unrec}}(t)\sigma(t)]_{\text{avg}}}{\omega\gamma_0^2} \tag{9}$$

and

$$G''_{\text{solid}}(\omega) = \frac{2(\dot{W}_{\text{diss,solid}}(\omega))_{\text{avg}}}{\omega\gamma_0^2} = \frac{2[\dot{\gamma}_{\text{rec}}(t)\sigma(t)]_{\text{avg}}}{\omega\gamma_0^2}. \tag{10}$$

Because the strain rates are additive, so too are the composite moduli

$$G'' = G''_{\text{solid}} + G''_{\text{fluid}}. \tag{11}$$

G''_{fluid} is proportional to the rate of dissipation of energy due to unrecoverable processes such as those accounted for by the dashpot element of a Maxwell fluid, as seen in Fig. 1(c). G''_{solid}, is proportional to the rate of dissipation of energy due to recoverable processes, such as those accounted for by the dashpot element of a Kelvin–Voigt solid where energy is dissipated, but all strains are recoverable, as seen in Fig. 1(d). Since each quantity is normalized by the total strain amplitude, neither is a function of *only* unrecoverable or recoverable strains, but the separation into two terms allows us to

compare them against one another, where the only difference between them is the numerator and, thus, the recoverable or unrecoverable aspect of each term. Because both viscoelastic solids and liquids can dissipate energy, we are forced to use another term to represent when flow takes place. We take the simple position that flow is associated with the acquisition of unrecoverable strain. The difference between viscoelastic solids and liquids is, therefore, not due to energy dissipation but due to the acquisition of unrecoverable strain.

This framework of recovery rheology allows us to determine the viability of the many ways of determining yield stress from oscillatory amplitude sweeps. Dinkgreve *et al.* identified three features that have been considered as indicators of yield stress. Typically, the data from an amplitude sweep are plotted in two ways, the first being the storage and loss modulus versus the applied amplitude, and the second being the measured amplitude versus the applied amplitude. One feature used to determine a yield point is the crossover between the storage modulus and loss modulus, termed "the yield point" by Shih *et al.* [32]. However, this crossover is not solely a measure of flow but rather represents when the rate of dissipation of energy through recoverable *and* unrecoverable processes surpasses elastic energy storage.

Two other features identified by Dinkgreve *et al.* require power-law fitting on logarithmic scales. One feature is the intersection of power-law fits of the storage modulus in the small-amplitude and large-amplitude limits, introduced by Rouyer *et al.* [33]. However, this method measures elastic energy storage normalized by the total strain, making it difficult to discern the effects from flow alone. The other feature is the intersection of power law fits of the stress amplitude dependence on the applied strain amplitude, introduced by Mason *et al.* [34]. Here, the strain amplitude represents a combination of recoverable and unrecoverable strains, making it difficult to separate flow from elastic behavior.

In addition to these three responses seen in an oscillatory amplitude sweep described by Dinkgreve *et al.*, there are three additional features commonly cited to determine yield stress. Mezger introduced a feature based on the point where the storage modulus deviates from linearity [35]. This method also relies on power-law fitting and requires a user-specified choice of how much deviation is considered significant, leading to different yield stress determinations. Another feature is the maximum of the product of the storage modulus and strain amplitude, incorrectly referred to as the elastic stress, introduced by Walls *et al.* [36]. This product is actually the average elastic energy divided by the total strain amplitude and, therefore, relates neither directly to flow nor elasticity. Donley *et al.* [19] recently investigated the overshoot in the loss modulus, a feature commonly associated with yield stress fluids, as discussed by Hyun *et al.* [37]. Donley *et al.* demonstrated that this overshoot arises from unrecoverable strains, but traditional amplitude sweeps carried out using only total strains and rates cannot differentiate between the two modes of energy dissipation.

As pointed out by Dinkgreve *et al.*, the methods commonly employed can yield significantly different numerical values for yield stress, and each method has its own limitations. These challenges range from experimental difficulties in applying low shear rates in steady shear experiments to uncertainties in determining crossover points and interpolations from imperfect data in oscillatory amplitude sweeps. The most common challenge is that many of the selected points do not clearly relate to a change from a no-flow to a flow condition. Despite the wide range of test protocols and challenges, there is still no single experiment universally used to determine yield stress for any given material.

C. Theoretical approaches to yield stress fluids

The earliest yield stress fluid model was proposed by Bingham [23], where the behavior of yield stress fluids was considered in the flowing state only. In this model, the stress response of a material is equal to a yield stress plus a "flow rule" that consists of a Newtonian stress. The works of Herschel and Bulkley (HB) and Casson [24,25] expanded upon this by changing the flow rule to be a power-law. The common link between these three models is that each only considers the yield stress fluid behavior while flowing and makes no explicit consideration for the response of the material below the yield stress.

Oldroyd made the distinction between the behavior above and below the yield stress separated by a single yield point but was careful to express that this required a quasi-static approach to the yield stress [10]. Along with the work of Prager, the treatment of yielding as two different responses separated by the yield stress became known as the Oldroyd–Prager formalism. Since then, many models have adopted the Oldroyd–Prager formalism even for transient cases. One such example is discontinuity in the stress response of a material at the transition point, as seen in models by Isayev and Fan or Puzrin and Holsby [38,39]. The issue of stress discontinuities was addressed in a model published by Saramito [40], which builds on the flow behavior of the Herschel–Bulkley model. The Saramito model describes the behavior below the yield stress as a viscoelastic solid with a mechanical analog represented by a Kelvin–Voigt solid, and the behavior above the yield stress as a viscoelastic fluid with a mechanical analog represented by a Maxwell fluid in parallel with a Newtonian dashpot, resulting in an Oldryod-B viscoelastic fluid. The transition between the two is mechanically represented by a frictional element, which represents instantaneous yielding. Thus, when stresses smaller than the yield stress are applied, all strain is acquired recoverably, and no flow occurs. When stresses larger than the yield stress are applied, strain will be acquired unrecoverably at a rate proportional to the applied stress and inversely proportional to the second viscous term. Since this model is mechanically represented by a spring in series with a dashpot that is only accessible above the yield stress, the constitutive equation is often written in terms of this stress, which is often called the polymeric stress, and the viscous stress, which are additive. The 1D version of the polymeric stress in the HB–Saramito model can be expressed as

$$\frac{\dot{\tau}_p}{G} + \max\left(0, \frac{|\tau_p| - \sigma_y}{k|\tau_p|^n}\right)^{1/n} \tau_p = \dot{\gamma}, \tag{12}$$

where τ_p and $\dot{\tau}_p$ are the polymeric stress and stress rate, respectively; G is a shear modulus; $\dot{\gamma}$ is the shear rate; and σ_y, k, and n are the yield stress, consistency, and power law index, as determined by a Herschel–Bulkley fitting of the steady shear flow curve. The total shear stress is written as

$$\sigma = \tau_p + \eta_f \dot{\gamma}, \tag{13}$$

where η_f is the flow viscosity in the Newtonian dashpot that allows for the acquisition of unrecoverable strain. It can be seen in Eq. (13) that the elastic stress represented in Eq. (12) is simply added to the viscous stress in the parallel dashpot. The function $\max(x, y)$ returns whichever value, x or y, is larger. If the magnitude of the applied stress in the elastic element is below the yield stress, Eq. (12), simplifies to that of a Hookean spring, which is then in parallel with a Newtonian dashpot, giving a Kelvin–Voigt viscoelastic solid. If the magnitude of the stress in the elastic element is larger than the yield stress, Eq. (12), simplifies to a Maxwell viscoelastic fluid, which is then in parallel with a Newtonian dashpot, giving an Oldryod-B fluid with a Herschel–Bulkley flow behavior. By using a function that chooses the maximum of two terms, it is clear that there is a binary transition separated by the yield stress. The HB–Saramito model is representative of the way the Oldroyd–Prager formalism is used today: treatment of yield stress fluids as having two different constitutive responses, separated by the yield stress, where acquisition of unrecoverable strain only occurs above the yield stress, even under transient conditions. This treatment of the Oldroyd–Prager formalism is where modern use of formalism diverges from the explicit description by Oldroyd.

Recently, Kamani, Donley, and Rogers (KDR) [20] proposed a model for yield stress fluids that goes beyond the Oldroyd–Prager formalism. In the KDR model, a single constitutive differential equation represents the material behavior above and below a single yield stress, with no instantaneous transition. This model was constructed on the basis of experiments that measured recoverable and unrecoverable strains [19]. Similar to the models utilizing Oldroyd–Prager, the KDR model utilizes only one yield stress, determined from a Herschel–Bulkley fitting of the flow curve to define its flow viscosity, which represents the behavior under quasi-static conditions. However, the flow viscosity term is dependent on the total strain rate, as opposed to just the unrecoverable strain rate typically associated with the steady-state flow. The experiments performed by Donley *et al.,* in which the recoverable and unrecoverable components were measured directly, showed a flow viscosity that depends on the sum of the two components of the strain rate. Since this flow viscosity is a function of the total strain rate, the acquisition of unrecoverable strain is aided by the rapid acquisition of recoverable strains. Within the KDR model, the timescale of deformation, therefore, becomes important. The KDR model is presented in a full tensorial manner elsewhere, but it can be represented in a simple 1D manner as

$$\sigma + \lambda(\dot{\gamma})\dot{\sigma} = \left(\frac{\sigma_y}{|\dot{\gamma}|} + k|\dot{\gamma}|^{n-1}\right)\left(\dot{\gamma} + \frac{\eta_s}{G}\ddot{\gamma}\right), \tag{14}$$

where the stress, stress rate, and Herschel–Bulkley parameters are the same as in Eq. (12). η_s is the viscosity associated with recoverable processes, and $\dot{\gamma}$ and $\ddot{\gamma}$ are the strain rate and strain acceleration, respectively. The elastic modulus determined in the linear regime is G. Meanwhile, λ is the relaxation time that depends on the total strain rate

$$\lambda(\dot{\gamma}) = \frac{1}{G}\left(\frac{\sigma_y}{|\dot{\gamma}|} + k|\dot{\gamma}|^{n-1} + \eta_s\right). \tag{15}$$

This model has been shown to predict gradual transitions typically observed in experimental studies of yield stress fluids, including all features of oscillatory amplitude sweeps, and the transient Lissajous responses associated with each amplitude, as well as steady shear startup and creep experiments [20].

D. Determination of flow

For yield stress fluids, the determination and description of the yield stress is the key challenge. Based on the Oldroyd–Prager formalism as used today, determining the yield stress is equivalent to asking when does a material flow. The answer to this question can be determined by a method that is susceptible to flow only. We take the position that a material is flowing when unrecoverable strain is being acquired. Within the recovery rheology framework, this is equivalent to seeking a method that is sensitive only to acquisition of unrecoverable strain. A test that identifies unrecoverable strain acquisition independently from recoverable strains was first shown by Lee *et al.* [41]. Lee *et al.* showed how viscoelastic materials would behave under application of an oscillatory stress, with an arbitrary phase angle, after an initial transience,

$$\sigma(t) = \sigma_0 \sin(\omega t + \psi), \tag{16}$$

where σ_0 is the amplitude of the sinusoidal stress wave, t is time, and ψ is the phase angle of the applied stress wave.

The component strains for viscoelastic fluids can be derived from the idealized cases of Hookean springs and Newtonian fluids. The response of a Hookean elastic material, seen in Fig. 1(a), to a phase-shifted sinusoidal stress can be simply determined by rearranging Eq. (3),

$$\gamma_{\text{rec}}(t) = \frac{\sigma_0 \sin(\omega t + \psi)}{G}, \tag{17}$$

which indicates that the recoverable strain of a spring will respond in an oscillatory manner, centered around zero.

The case of a generalized Newtonian fluid, seen in Fig. 1(b), subjected to the same stress protocol, by contrast, is

$$\gamma_{\text{unrec}}(t) = \int_0^t \dot{\gamma}_{\text{unrec}}(\hat{t})\, d\hat{t} = \int_0^t \frac{\sigma_0 \sin(\omega \hat{t} + \psi)}{\eta}\, d\hat{t}, \tag{18}$$

where $\hat{t}$ is a dummy variable of integration, and the bounds are set for any period of time from 0 to t, where the initial

condition of the system is unstrained, so that $\gamma(0) = \gamma_{rec}(0) = \gamma_{unrec}(0) = 0$. From this integration, we see the steady-state unrecoverable strain as a function of time [41,42],

$$\gamma_{unrec}(t) = \frac{\sigma_0}{\omega\eta}\cos(\psi) - \frac{\sigma_0}{\omega\eta}\cos(\omega t + \psi). \tag{19}$$

At the steady state, the unrecoverable strain response to a phase-shifted sinusoidal stress is also oscillatory, but there is a constant term about which this oscillation is centered. This constant was termed the strain shift by Lee *et al.* Since viscoelastic materials acquire recoverable and unrecoverable strains in a linear sum, the constant term in Eq. (19) is the strain shift for a viscoelastic fluid

$$\gamma_{s,VE} = \frac{\sigma_0}{\omega\eta_0}\cos(\psi). \tag{20}$$

This strain shift is dependent on three parameters controlled by the experimenter, the angular frequency, the stress amplitude, and the phase of the applied stress, and one material parameter, the flow viscosity. Following the work of Lee *et al.*, Hassager [42] analyzed the startup response of a viscoelastic material and arrived at the same expression in Eq. (20) for the steady-state response of a viscoelastic fluid, and recently, Ogunkeye *et al.* showed that the steady-state strain shift will also be independent of any instrumental inertia [43].

Under a phase-shifted oscillatory stress, any material that responds in a solidlike manner, where all strain is acquired recoverably, will oscillate about the position defined as zero strain before the experiment began. In contrast, any liquidlike response will oscillate about a constant nonzero value. Therefore, strain shifts determined from stress-controlled oscillations can be used to identify unrecoverable acquisition of strain and by extension whether flow has taken place over the timescale set by the frequency of the oscillation.

In the context of a phase-shifted sinusoidal wave, the phase angle determines the starting point of the wave within its period. For instance, a phase angle of $\psi = \pi/2$ corresponds to a sine wave shifted by half a period, which is equivalent to a cosine wave. The convention of applying a cosinusoidal stress to a material during stress-controlled oscillations has been suggested due to the mathematical simplicity of Fourier and harmonic analysis [44,45]. However, the strain shift is a parameter that carries physical significance of how much a material has flowed [41]. As shown in Eq. (20), if the applied stress is cosinusoidal, the strain shift equals zero, and the physical information it carries becomes inaccessible. Considering the physical interpretation of the strain shift allows the experimenter to make more informed decisions. They may choose to avoid strain shift by applying a cosinusoidal stress, or they can maximize the strain shift by applying a sinusoidal stress, or they can select a value in between to achieve the desired outcome.

While Lee *et al.* were the first to design experiments specifically to measure the strain shift [41], the idea was introduced in a problem by Pipkin in his lectures and textbook on viscoelasticity [46]. Despite Pipkin posing the problem in 1986, and other observations of this strain shift phenomenon [42,45,47–51] modern rheological software, under stress-controlled oscillations, will subtract this value and artificially set the strain to oscillate about zero. This "behind-the-scenes" subtraction requires researchers to circumvent the built-in experimental protocols to access the full unadulterated material response. In fact, we believe one of the reasons for the sparse discussion of this phenomenon is due to the fact that this term is subtracted out before researchers even know it is there.

As shown by Lee *et al.,* the experimental protocol to determine strain shift provides a repeatable method to determine when unrecoverable strain has been acquired and to determine the viscous properties of soft materials. For yield stress fluids, this presents an opportunity to directly test the hypothesis set out by the Oldroyd–Prager formalism as it is used today. Any model or discussion that invokes the ideas of the Oldroyd–Prager formalism for transient experiments would expect to have zero strain shift for stress amplitudes below the yield stress, due to the treatment of the pre-yielded behavior as being a purely recoverable solid. Strain shift experiments, therefore, provide a clear and unambiguous indicator of when unrecoverable strain is acquired and, therefore, when flow occurs.

In this work, we measure the strain shift for a well-studied yield stress fluid and determine the strain shift across a range of stress amplitudes ranging from well below to well above the yield stress as determined by fitting the flow conditions to the Herschel–Bulkley model in the quasi-static limit. We compare these results to predictions of the HB–Saramito and KDR models. We then connect the strain shift to the fluidlike loss modulus introduced by Donley *et al.* [19] and derive an expression for the recoverable and unrecoverable rates of dissipation of energy as a function of strain shift. Determination of these parameters has previously been attainable only through iterative recovery measurements. Our new approach, therefore, significantly reduces experimentation time. These results are compared against measures obtained from iterative recovery tests to validate our expressions and to highlight the greater impact that measuring strain shift provides.

II. MATERIALS AND METHODS

Strain shift experiments were performed on a TA Instruments DHR-3 torque-controlled rheometer using the protocol illustrated in Fig. 2. The geometry used was a 40mm parallel plate, with 220 grit sandpaper adhered to both surfaces with double sided tape, which eliminates wall slip. Since the TRIOS software will report any strain response as oscillating about zero when using the built-in oscillatory functions, strain shift experiments were performed under the arbitrary wave function in the TRIOS software. Each iteration of the experiment consists of three steps: the first steps acts to zero the strain and ensure a consistent starting point and is enacted by applying zero shear stress for a time t_{wait}; the second step is the application of the sinusoidal stress with desired amplitude, frequency, and phase for a duration of t_{test}; the third and final step in each iteration is the recovery step, where zero shear stress is applied again, and the material is allowed to recover and return to equilibrium,

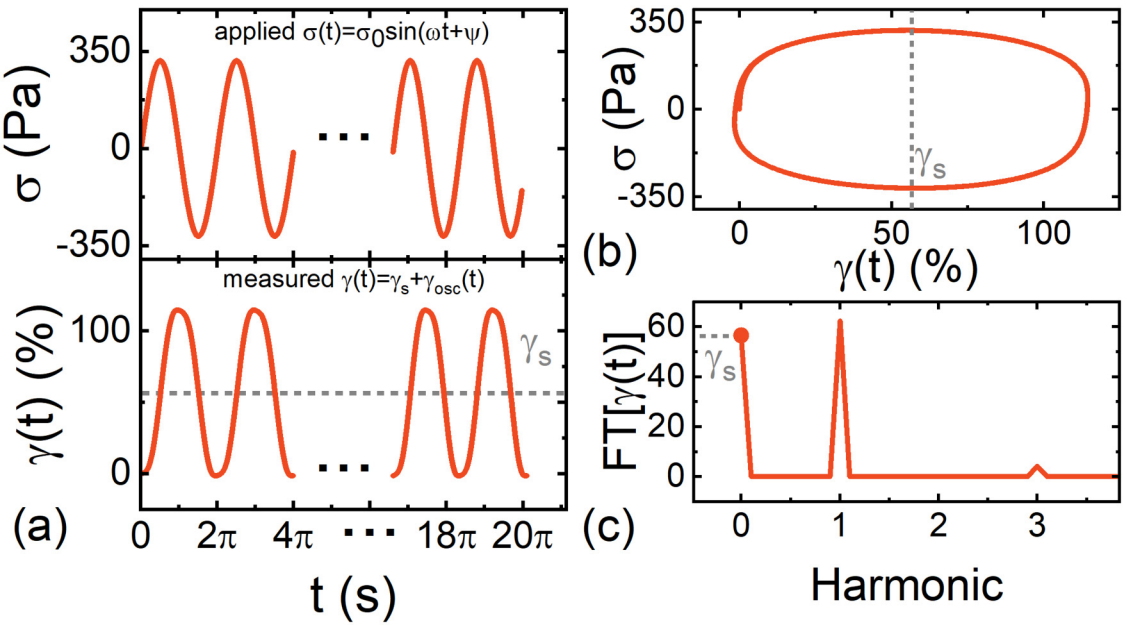

FIG. 2. (a) Arbitrary stress applied to a material (top left), and measured strain response with dotted line showing oscillation about a nonzero value (bottom left), (b) Lissasjous curve of stress versus strain showing strain centered about a nonzero value, and (c) Fourier transform of the strain response, highlighting the zeroth harmonic, giving the numerical value of the strain shift.

for t_{recovery}. For our samples, 20 seconds was determined to be sufficient for the material to recover at least 95% of its total recoverable strain. Each of these tests is then repeated in the forward ($\sigma_0 > 0$) and reverse ($\sigma_0 < 0$) directions to account for possible instrument drift. Each pair is repeated three times per set of test parameters. The data were analyzed by calculating the discrete Fourier transform (DFT) of each period, and the parameters were averaged based on the last three periods of applied stress and measured strain. From the DFT, we can determine the storage and loss modulus as the first harmonic terms, as well as the strain shift, which is the zeroth harmonic term of the strain response. For every new test parameter, the results from the first of three pairs is ignored to ensure repeatable results. A graphical representation of the test protocol for a given stress amplitude, and the first step of the analysis, can be seen in the supplementary material [58].

The behavior of a well-studied yield stress fluid was investigated. Carbopol 980 NF (C980) produced by Lubrizol, was dissolved in propylene glycol (PG), at three different weight percents (1.6%, 1.8%, and 2.0%). The C980 was added to PG, and mixed using a THINKY orbital mixer at 2000 rpm for 60 min, and then let rest for at least 24 h prior to any testing. All rheological measurements were performed at 25 °C. The steady shear flow curve, amplitude sweep, and linear regime frequency sweep for the 1.6% C980 in PG are shown in Fig. 3. From the linear regime response, we determine the shear modulus and the solid viscosity. From the steady shear flow curve, we fit the data to obtain Herschel–Bulkley parameters for all three concentrations, which are shown in a table in the supplementary material [58]. We refer to these flow curve parameters as representing the quasi-static behavior of the material, as they are representative of steady-state behavior and are not affected by any transience. In additional, our materials behave qualitatively similar to other materials that have the yield stress where slip is not seen [52]. The star polymer glasses studied by Erwin *et al.* also dissipate energy below the yield stress. This energy dissipation was attributed to the free or dangling ends of the stars. The Carbopol we have studied is also likely to have some dangling ends, providing a possible or partial mechanism for energy dissipation at small stresses. These characterizations were performed on an Anton Paar MCR 302 rheometer under displacement control using the automatic rate controller. The geometry used for the characterizations was a 50 mm parallel plate, with 220 grit sandpaper adhered to both surfaces using double sided tape to avoid slip.

III. STRAIN SHIFTS IN YIELD STRESS FLUIDS

We show in Fig. 4 the results of our strain shift experiment on 1.6% Carbopol at 0.5 rad/s. We show in Fig. 4(a), the traditional storage and loss modulus as a function of the stress amplitude normalized by the yield stress as determined by the Herschel–Bulkley fitting of the steady-shear flow curve. When compared to the data of Fig. 3, where the data are plotted against strain amplitude, we see many features common to yield stress fluids: a linear regime where $G' > G''$, an overshoot in G'' at intermediate amplitudes, and a point at which G' and G'' crossover. The dashed vertical line at $\sigma_0/\sigma_{y,\text{HB}} = 1$ is a visual marker that indicates the yield stress. We compare the amplitude dependence of the dynamic moduli to the strain shift, as seen in Fig. 4(b). Our measurements of strain shift span eight decades of strain, from 10^{-5} to 10^{3}, across four decades in stress amplitude. In addition to the measurements, the predictions of the HB–Saramito model and the KDR model are also shown in Fig. 4(b).

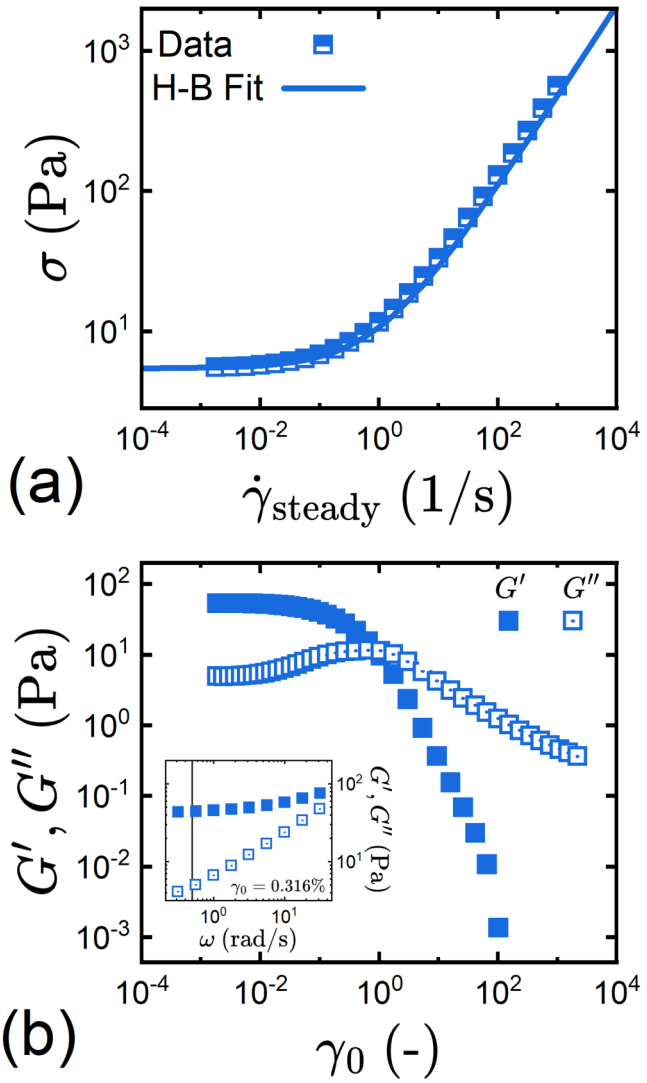

FIG. 3. Data for 1.6% Carbopol 980 in PG, (a) steady shear flow curve determined from a series of steady-shear startup tests with Herschel–Bulkley fitting. (b) Amplitude sweep at an angular frequency $\omega = 0.5$ rad/s equal to the vertical line in the inset. The inset is a linear regime frequency sweep at $\gamma_0 = 0.0316\%$.

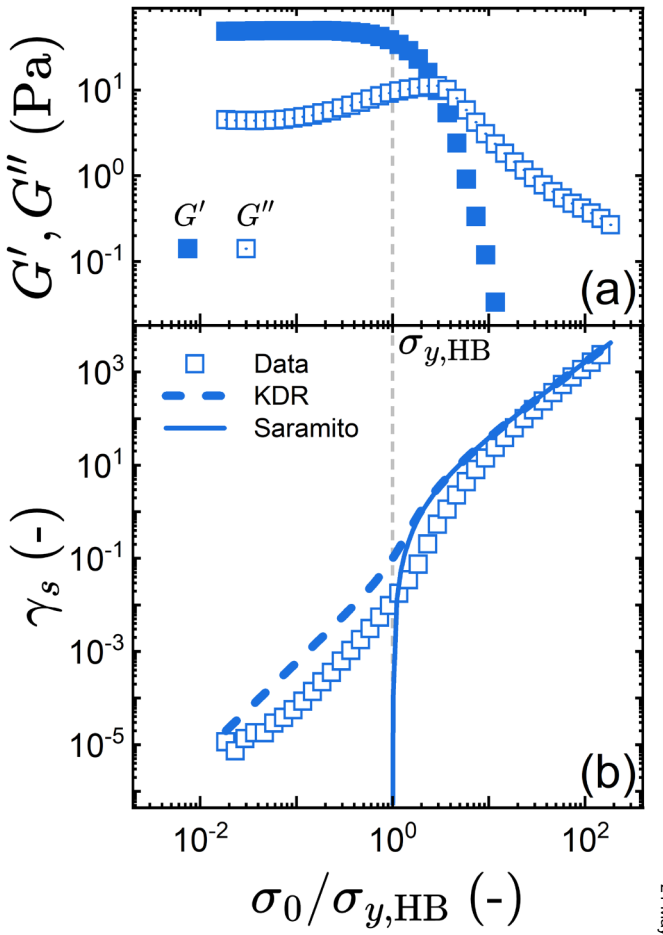

FIG. 4. Data for 1.6% C980 in PG at $\omega = 0.5$ rad/s. (a) Amplitude sweep determined from the oscillatory response of waveform versus stress amplitude normalized by the Herschel–Bulkley yield stress. (b) Symbols show strain shift (nonoscillatory response of waveform). Dotted line shows KDR model predictions of strain shift, while solid lines show the HB–Saramito model prediction of strain shift all versus stress amplitude normalized by the Herschel–Bulkley yield stress.

The major conclusion to be drawn from the strain shift data shown in Fig. 4(b) is that we are able to measure strain shifts at all stress amplitudes, even those well below the yield stress. This means that there is unrecoverable flow occurring below the yield stress. We also see that the strain shift is a continuous function of the stress amplitude, which is notable for the lack of an abrupt transition as the yield stress is crossed. The expectation based on the Oldroyd–Prager formalism, exemplified by the HB–Saramito model shown as solid lines in Fig. 4(b), is that there is no unrecoverable flow below the yield stress and so the strain shift should be zero. This expectation ignores the distinction made by Oldroyd that the binary nature of the yield stress is only true for the quasi-static case where the yield stress is approached infinitesimally slowly. Our data, collected over finite time scales, show that unrecoverable strain is acquired continuously across the range of applied stresses, both above and below the yield stress.

We observe that the experimentally measurable strain shift does not abruptly change or go to zero as the yield stress is approached or crossed. In fact, there is no obvious transition in the unrecoverable behavior as the yield stress is crossed, and it appears as though the only limitation in determining smaller strain shifts is technological. We reliably determine strain shifts as small as 10^{-5} strain units, or 1000th of 1%, at stress amplitudes around a 100th of the yield stress. As small as these strain shifts are, they are 3 orders of magnitude larger than the lower limit of the displacement resolution for the DHR3, which is discussed in detail in the supplementary material [58].

In Fig. 4, we display the strain shift as a function of the applied stress amplitude normalized by the yield stress determined under quasi-static conditions. To explore the functional dependence of the strain shift on the stress and strain amplitudes, in Fig. 5, the strain shift is plotted as a function of (a) the measured strain amplitude and (b) the normalized stress amplitude. While the full KDR model requires numerical solutions, scalings can be found in the small and large amplitude limiting cases. These are also shown in Fig. 5 and are derived below.

A. Large-amplitude scaling

For the case of stress amplitudes much larger than the yield stress, a yield stress fluid may be considered to flow like a generalized Newtonian fluid. By writing the flow viscosity as a ratio of the stress amplitude and rate amplitude in Eq. (20), the strain shift can be written as

$$\gamma_s = \frac{\sigma_0}{\omega\eta_{\text{flow}}}\cos(\psi) = \frac{\sigma_0}{\frac{\omega\sigma_0}{\dot{\gamma}_0}}\cos(\psi) = \gamma_0\cos(\psi). \tag{21}$$

This result was derived from Lee at al. for the case of viscoelastic materials but is rewritten here to show the strain amplitude dependence more clearly. When a sinusoidal stress is applied, the phase angle is zero, and the cosine of the phase angle is one. The strain shift, therefore, scales linearly with the strain amplitude. The data of Fig. 5 support this scaling.

We can obtain the scaling of the strain shift with the stress amplitude by inserting the functional form of the stress amplitude on the strain amplitude into Eq. (21). The stress response of yield stress fluids in the large stress limit is commonly represented by the Herschel–Bulkley equation

$$\sigma(\dot{\gamma}) = \sigma_y + k\dot{\gamma}^n. \tag{22}$$

We can solve for the strain rate, for an applied sinusoidal stress,

$$\dot{\gamma} = \left(\frac{\sigma_0\sin(\omega t + \psi) - \sigma_y}{k}\right)^{1/n}. \tag{23}$$

Since we seek the relationship between the stress amplitude and strain amplitude, we can determine the amplitude of the strain rate by taking the maximum of the right hand side, simplifying the expression to

$$\dot{\gamma}_0 = \left(\frac{\sigma_0 - \sigma_y}{k}\right)^{1/n}. \tag{24}$$

Typically, in the large stress limit, the oscillatory strain response is not purely sinusoidal. However, we can approximate the amplitude of the strain rate as being equal to the amplitude of the strain times the frequency. Therefore,

$$\gamma_0 = \frac{1}{\omega}\left(\frac{\sigma_0 - \sigma_y}{k}\right)^{1/n}. \tag{25}$$

The expression for the strain amplitude for a yield stress fluid under a large-amplitude stress-controlled oscillation can be placed into Eq. (21),

$$\gamma_{s,\text{large}} = \gamma_{0,\text{large}}\cos(\psi) = \left(\frac{\sigma_{0,\text{large}} - \sigma_y}{k}\right)^{1/n}\frac{\cos(\psi)}{\omega}, \tag{26}$$

which allows us to predict that we should see a scaling of the strain shift with the stress amplitude as having a slope of n_{HB}^{-1} on a log-log plot. This prediction of the scaling matches the data seen in Fig. 5(a).

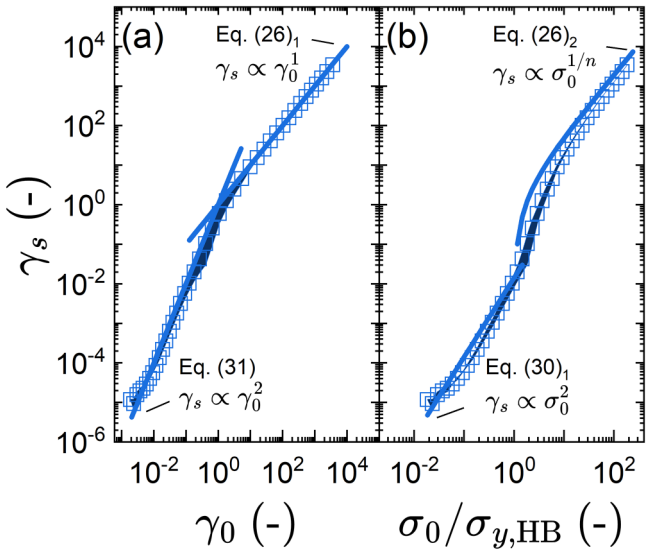

FIG. 5. Strain shift response as a function of (a) normalized stress amplitude and (b) measured strain amplitude for 1.6% C980 in PG at $\omega = 0.5$ rad/s. The filled in area represents the space between the upper and lower error bars between three trials. Scaling for small-amplitude and large-amplitude are shown, which are fully derived in Eqs. (26), (30), and (31).

B. Small-amplitude scaling

While the large-amplitude scaling follows an approach that is essentially no different from the case derived by Lee *et al.* and Hassager with a rate-dependent viscosity, and would be the same for models that follow the Oldroyd–Prager formalism, the small amplitude case is less obvious. According to the Oldroyd–Prager formalism, there should be no acquisition of unrecoverable strain below the yield stress and so there should be no strain shift. Our experiments show this not to be true, and we observe strain shift at all stress amplitudes we have applied. There are clearly two regions of material behavior that can be observed in our raw data with a continuous acquisition of unrecoverable strain across all applied stress amplitudes.

Clearly, applying Oldroyd–Prager thinking to the small amplitude case would not result in an accurate representation of our experimental data. Instead, we turn to the KDR model, which has accurately described other rheological features of yield stress fluids. We again approximate the strain rate amplitude as being the strain amplitude times the frequency, and we take the flow viscosity using the low-rate limit of the Herschel–Bulkley model seen in Eq. (22). This reduces the Herschel–Bulkley model to the yield stress term only, as the flow rule term becomes negligible at low rates. The flow viscosity at small stresses can be expressed as

$$\eta_{\text{flow,small}} = \frac{\sigma_y}{\omega\gamma_{0,\text{small}}}. \tag{27}$$

Below the yield stress, this flow viscosity is dependent on the timescale of experimentation, accounted for by the

angular frequency. A time-dependent flow viscosity below the yield stress has also been seen for the case of non oscillatory tests, such as by Barnes and Walters, as well as Møller *et al.* [26,53], who showed that measurement of the viscosity at small stresses will continue to increase as a function of experiment time. However, as noted in the work by Møller *et al.*, the viscosities measured are consistent with those of a Kelvin–Voigt viscoelastic solid at finite times that are independent of stress or rate amplitude and make no distinction between recoverable and unrecoverable acquisition of strain [53,54]. In contrast, a Herschel–Bulkley behavior below the yield stress, as in the KDR model, results in a flow viscosity shown in Eq. (27) that is dependent on both recoverable and unrecoverable strain rates. The viscosity related to the recoverable strain rate will follow the rate independence that is presented by Møller *et al.,* but the viscosity related to unrecoverable flow will be inversely dependent on the rate.

Since we are in the limit of small stresses, the strain amplitude response will be dominated by the recoverable component, allowing us to approximate the total strain amplitude as the ratio of the stress amplitude and the elastic modulus,

$$\gamma_{0,\text{small}} \approx \frac{\sigma_{0,\text{small}}}{G}. \tag{28}$$

Inserting Eq. (28) into Eq. (27), we obtain a new expression for the flow viscosity,

$$\eta_{\text{flow,small}} = \frac{G\sigma_y}{\omega\sigma_{0,\text{small}}}. \tag{29}$$

It can be seen in Eq. (29) that for a yield stress fluid under a fixed stress amplitude oscillation, the flow viscosity scales inversely with the frequency. That is, the faster the oscillation, the lower the viscosity, even below the yield stress. This expression directly relates to the quasi-static case presented by Oldroyd, since in the limit of zero frequency, or infinite time, the viscosity will be infinite and the material will not flow below the yield stress. The importance of Eq. (29) is that it makes it clear that for any real timescale, there is a finite flow viscosity that will lead to some small amount of flow at any stress.

We can now take this flow viscosity from Eq. (29) and determine the strain shift by inserting it into (21),

$$\gamma_{s,\text{small}} = \left(\frac{\sigma_0}{\sigma_y}\right)\left(\frac{\sigma_0}{G}\right)\cos(\psi) = \left(\frac{\sigma_0}{\sigma_y}\right)\gamma_0\cos(\psi). \tag{30}$$

The frequency dependence that may have been expected in this term is absent because both the flow viscosity and the strain shift are inversely dependent on the frequency. For the strain shift, lower frequencies mean the material has more time to move further away from the initial position, while the flow viscosity gets larger at lower frequency. The two effects thus compete and cancel each other out. Unlike the expression we obtained for the viscosity at small stresses, shown as Eq. (29), the expression for the strain shift under small stress amplitudes shown as Eq. (30) does not contain the Oldroyd–Prager behavior as a limiting case. In fact, we predict that the strain shift for yield stress fluids subjected to small sinusoidal stresses is *independent* of the frequency, which means that yield stress fluids will *always* flow below the yield stress, even if only a little bit.

The small-amplitude scaling shown in Eq. (30) looks very similar to the large-amplitude scaling shown in Eq. (26). In the large-amplitude case for a sinusoidal stress, the strain shift is equal to the strain amplitude, while in the small amplitude case the strain shift is equal to the strain amplitude times the stress amplitude normalized by the yield stress, which is the term the data have been plotted against in Figs. 4 and 5(b). The form of Eq. (30) also allows us to make another interesting observation, that for a sinusoidal stress we should expect the strain shift to be a fraction of the total strain given by σ_0/σ_y. For any nonzero stress amplitude, no matter how small it is compared with the yield stress, we expect some amount of unrecoverable flow to take place.

In addition, if we invoke Eq. (28) and express the yield stress as the product of the modulus and the yield strain $\sigma_y = G\gamma_y$, which is the expected response at small rates in the KDR model [20], we can determine the strain amplitude dependence of the strain shift as

$$\gamma_{s,small} = \frac{\gamma_{0,\text{small}}^2}{\gamma_y}\cos(\psi). \tag{31}$$

The small-amplitude strain shift is, therefore, predicted to scale with the square of the strain amplitude as long as the yield strain is constant, which holds true in the small-rate limit [20]. The agreement between the data and Eq. (31) rules out the possibility of a Newtonian slip layer in this material, as this would result in the strain shift scaling with the measured strain amplitude, as in the large-amplitude case. The scalings predicted by Eqs. (30) and (31) agree with the data, as shown in Fig. 5, meaning a full solution of the KDR model is not required.

In addition to the single exemplary case presented so far, we also show in Fig. 6 the strain shift results for other Carbopol concentrations and other applied angular frequencies. In Fig. 6(a), we show the strain shift for three concentrations and two frequencies as a function of the measured strain amplitude. Based on Eq. (31), we expect the small amplitude scaling to have a slope of two on a log-log plot, which is what we see for all three concentrations. In fact, the quality of the overlay when shown as functions of the strain amplitude implies that the yield strain for all three concentrations is identical. At large amplitudes, we expect a generalized Newtonian response, as suggested by Eq. (21), which is indicated by a slope of one.

In Fig. 6(b), we show the strain shift for the three concentrations and two frequencies as a function of the applied stress amplitude. For large stress amplitudes, based on Eq. (26), we expect the strain shift for each to be different, depending on the Herschel–Bulkley parameters, which is what is seen. The log-log scalings depend specifically on the power-law index n, which is why the large amplitude

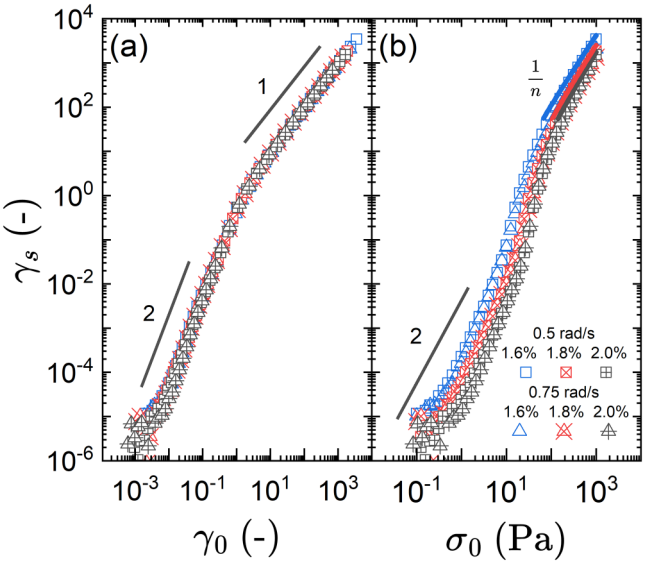

FIG. 6. Strain shift as a function of (a) measured strain amplitude and (b) applied stress amplitude for three concentrations of C980 in PG at two frequencies showing 1.6% C980 (blue and open) 1.8% C980 (red and diagonal crosses) and 2.0% C980 (black crosses), and frequencies of 0.5 (squares) and 0.75 rad/s (triangles), with lines of the log-log slope shown.

behavior of each concentration has different slopes. For the case of small stress amplitudes, Eq. $(30)_1$ predicts a squared scaling of the strain shift with respect to the stress amplitude, which is shown with the log-log slope of 2.

IV. BEYOND YIELD STRESS FLUIDS

Up to this point, we have focused on determining the strain shift response of yield stress fluids and have shown that they will always acquire unrecoverable strain. They, therefore, flow below their yield stress. Lee *et al.* [41] and Hassager [42] have previously discussed the phenomenon of strain shift for viscoelastic fluids. Since those studies, recovery rheology has been shown to solve other problems also, in particular, the expositions of Donley *et al.* [19] and Kamani *et al.* [20] that showed how the amplitude sweep response of yield stress fluids can be understood in terms of one storage modulus and two components of the loss modulus. The two components of the loss modulus correspond to energy dissipation through recoverable processes, such as changes of conformation, and unrecoverable processes, such as center of mass motion. In a follow up work, Kamani *et al.* [21], showed how an instantaneous Deborah number can be defined in terms of recoverable and unrecoverable components. The work of Lee *et al.* clearly established that the strain shift comes from unrecoverable processes alone, and so we now investigate what link, if any, exists between the strain shift measure and the fluid component of the loss modulus.

By carefully performing the strain shift experiments at each stress amplitude, we can gain the same understanding of a traditional amplitude sweep with the oscillatory response of the material, along with the average recovery metrics for the rate of dissipation of energy. From the oscillatory portion of the strain response, one can determine the storage and loss modulus, as described above and elsewhere [55,56]. The derivations of the signal processing, and determination of the moduli are not novel, but are replicated in the supplementary material [58] for completeness for the case of a sinusoidal stress. We can directly recreate the amplitude sweep from our experiments, with additional information from the strain shift.

When stress-controlled tests are discussed from the theoretical perspective, the response is often shown as a compliance rather than a modulus. However, rheometry software typically shows moduli for stress-controlled amplitude sweeps. By carefully considering the energetic definitions, one can convert between moduli and compliance across both the linear and nonlinear material responses. Due to the convention of compliance for stress-controlled tests, we will continue our derivations in compliance and convert to modulus as necessary.

We begin this discussion by examining loss and storage compliance in terms of energy dissipation and storage,

$$J'(\omega) = \frac{4(W_{\text{stored}}(\omega))_{\text{avg}}}{\sigma_0^2} = \frac{2[\sigma(t)\gamma(t)]_{\text{avg}}}{\sigma_0^2}, \tag{32}$$

$$J''(\omega) = \frac{2(\dot{W}_{\text{diss.}}(\omega))_{\text{avg}}}{\sigma_0^2\omega} = \frac{2[\sigma(t)\dot{\gamma}(t)]_{\text{avg}}}{\omega\sigma_0^2}. \tag{33}$$

Equations (32) and (33) are the direct parallels of the moduli terms expressed in Eqs. (7) and (8), which are all forms we attribute to Tschoegl [31]. In the Introduction, we also showed the fluidlike and solidlike components of the loss modulus, as derived by Donley *et al.* Similar expressions exist for the loss compliance, but instead of normalizing by the total strain amplitude, the energetic terms are normalized by the stress amplitude

$$J''_{\text{solid}}(\omega) = \frac{2(\dot{W}_{\text{diss,solid}}(\omega))_{\text{avg}}}{\omega\sigma_0^2} = \frac{2[\dot{\gamma}_{\text{rec}}(t)\sigma(t)]_{\text{avg}}}{\omega\sigma_0^2}, \tag{34}$$

$$J''_{\text{fluid}}(\omega) = \frac{2(\dot{W}_{\text{diss,fluid}}(\omega))_{\text{avg}}}{\omega\sigma_0^2} = \frac{2[\dot{\gamma}_{\text{unrec}}(t)\sigma(t)]_{\text{avg}}}{\omega\sigma_0^2}. \tag{35}$$

These can now be applied directly to the case of our experimental strain shift procedure. There is an equivalence in the concepts addressed by Eq. (35), which represents the portion of the loss compliance that comes from unrecoverable rate of dissipation of energy, and the strain shift, which also only comes from unrecoverable processes. To develop a formal expression that links the two measures, we begin with the form shown in Eq. (4) for the unrecoverable strain rate and our sinusoidal stress to calculate the fluid component of the loss compliance from Eq. (35). Since the average of any squared sine wave for an integer number of periods is equal to $\frac{1}{2}$, we see

$$J''_{\text{fluid}}(\omega) = \frac{2}{\omega\sigma_0^2}\left(\frac{\sigma_0^2\sin^2(\omega t+\psi)}{\eta_{\text{flow}}}\right)_{\text{avg}} = (\omega\eta_{\text{flow}})^{-1}. \tag{36}$$

We see from Eq. (36) that the fluid component of the loss compliance is equal to the inverse of the angular frequency times the flow viscosity. This flow viscosity can be expressed in terms of the strain shift as seen in Eq. (21). Inserting that form into Eq. (36), we see

$$J''_{\text{fluid}}(\omega) = \frac{\gamma_s}{\sigma_0 \cos(\psi)}. \tag{37}$$

A similar process can be followed to calculate the connection between the flow viscosity and the fluid component of the loss modulus. In this case, we find

$$G''_{\text{fluid}} = \frac{2}{\omega\gamma_0^2}\left(\frac{\sigma_0^2 \sin^2(\omega t + \psi)}{\eta_{\text{flow}}}\right)_{\text{avg}} = \frac{\sigma_0^2}{\gamma_0^2}(\omega\eta_{\text{flow}})^{-1}, \tag{38}$$

and the connection between the fluid component of the loss modulus and strain shift follows as

$$G''_{\text{fluid}} = \frac{\sigma_0 \gamma_s}{\gamma_0^2 \cos(\psi)}. \tag{39}$$

We, therefore, have the link we sought between the strain shift measure, γ_s, and the fluid component of the loss modulus, G''_{fluid}. The solid component of the loss modulus follows directly from the additive nature of the loss modulus components shown in Eq. (11), by subtracting the fluid component from the total

$$G''_{\text{solid}} = G'' - G''_{\text{fluid}}. \tag{40}$$

These two equations make it clear that if you apply a sinusoidal stress to any material and obtain the raw strain response including the strain shift, it is possible to distinguish between the components of the dynamic loss modulus without any extra experimentation.

The definitions of the compliance and moduli shown above are well defined for all applied phase angles of the stress except when cosinusoidal waves are used. In the case of a cosinusoidal stress, it is not possible to determine a strain shift and, therefore, the rate of dissipation of energy due to acquisition of unrecoverable strains through this experimental protocol. This loss of information about the flow behavior of a material constitutes a clear reason to avoid the use of a cosinusoidal stress.

We compare, in Fig. 7, the components of the loss modulus determined from the strain shift as well as from iterative recovery experiments. In Fig. 7(a), the total loss modulus, as well as the fluid and solid components of the loss modulus calculated from the strain shift experiment, are shown as a function of the total strain amplitude. In Fig. 7(b), we show the solid component of the loss modulus due to recoverable rate of dissipation of energy, and in (c), we show the component of the loss modulus due to unrecoverable rate of dissipation of energy, comparing the results obtained from the strain shift experiment to those measured via iterative recovery tests. The measure obtained from the strain shift matches that obtained from the iterative recovery

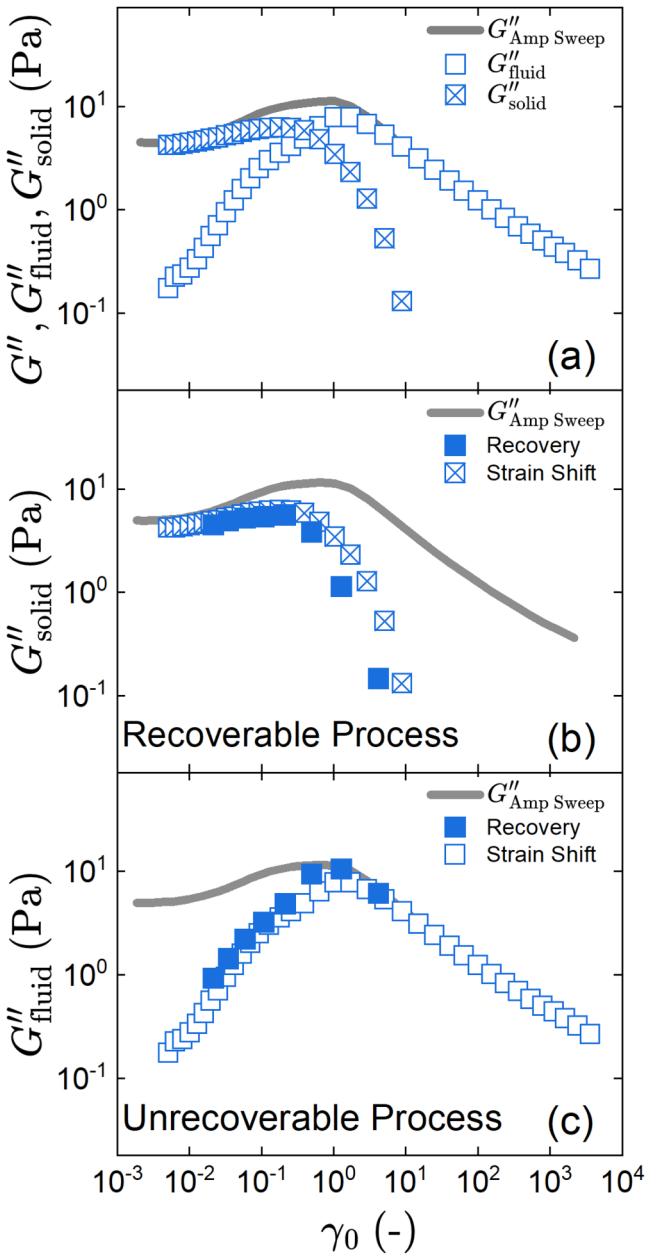

FIG. 7. Data for 1.6% C980 in PG at $\omega = 0.5$ rad/s. (a) Both components of the loss modulus determined via the strain shift experiment, and the total loss modulus as a gray line. (b) Component of loss modulus from recoverable processes, (G''_{solid}) and (c) component of loss modulus from unrecoverable processes (G''_{fluid}) determined from the both the strain shift experiment (cross symbols) and iterative recovery tests (solid symbols). The solid line is the total dynamic loss modulus.

experiments. Results for other concentrations and angular frequencies are shown in the supplementary material [58].

Stress-controlled oscillatory shear tests, therefore, provide a way to measure strain shift and calculate the components of the loss modulus as seen in Eqs. (38) and (40). Previously, iterative recovery experiments have been required to determine these average metrics. While the strain shift gives us clear access to averaged measures, as shown above, the strain shift experiment cannot give access to the transient information that iterative recovery experiments provide that helps explain the transient nature of yielding [21]. However, the strain shift experiment can achieve the same average

information as iterative recovery experiments, while significantly reducing the number of experiments required and, therefore, the time.

V. CONCLUSIONS

While it is expected that yield stress fluids flow above their yield stress, we have shown through strain shift experiments that they also flow below their yield stress over finite timescales. The commonly applied Oldroyd–Prager formalism, and any model that adheres to it, predicts no strain shift below the yield stress. This measure of acquisition of unrecoverable strain is distinct from the dissipation of energy associated with recoverable processes displayed by a viscoelastic solid. Energy dissipation below the yield stress has been reported for yield stress fluids previously [54,57], but flow and dissipation of energy are different phenomena. Flow implies an acquisition of unrecoverable strain, while viscoelastic solids and liquids both dissipate energy. Since a Kelvin–Voigt viscoelastic solid only acquires strain and dissipates energy recoverably, and unrecoverable flow is shown to occur below the yield stress by the strain shift experiment, yield stress fluids are not simply viscoelastic solids below the yield stress.

In Eq. (30), we show that yield stress fluids will flow across all stress amplitudes, independent of frequency and that the strain shift measured at small stress amplitudes is a simple fraction of the total strain given by the ratio of the applied stress amplitude to the yield stress, $\gamma_s/\gamma_0 = \sigma_0/\sigma_y$. The no-flow condition of Oldroyd–Prager, and the common description of yield stress fluids only flowing above the yield stress, only holds true for the quasi-static case. In all physical experiments, yield stress fluids will flow below the yield stress. We have derived expressions that match our experimental observations from the KDR model, which contains a well-defined yield stress. From the results we have obtained in this study, we can now interpret the yield stress in Carbopol and the KDR model as the stress below which no flow occurs only in the quasi-static case. Over finite timescales, and across all stress amplitudes, above and below the yield stress, yield stress fluids flow.

Stress-controlled rheology, through strain shift experiments can be used to determine metrics previously requiring iterative recovery procedures. We show in Eqs. (37) and (39) that the fluid component of the loss modulus contains the same physics as the strain shift. The component moduli determined by strain shift are compared directly to those measured using iterative recovery rheology, with great success. From the protocol described in this work, stress-controlled oscillatory shear is able to give researchers the average measured determined by recovery rheology. However, any transient information still requires the full recovery rheology protocol.

Our conclusions are reminiscent of the discussion put forward by Barnes and Walters regarding the yield stress myth [26] but are crucially distinct in reasoning and conclusion. Their argument is that if one could measure at low enough shear rates and wait long enough, a Newtonian plateau would be observed in the viscosity. Our results are distinct from this perspective, and add a new chapter to the discussion. Our work shows that at low enough constant shear rates at long enough times, yield stress fluids *do not* flow. However, our results show that it is possible for a constitutive relation to have a well-defined yield stress, below which no flow occurs in the quasi-static case but that still flows under transient conditions as a result of transient kinematics acting upon such a relation. From this perspective, the Oldroyd–Prager-style yield stress, which must be exceeded for any flow to occur, is indeed a myth.

The derived results of strain shift scalings may be specific to simple yield stress fluids, which show no time dependence in their behavior. However, given the generality of the features observed in Carbopol that are common across other YSFs, we expect the phenomenon of the strain shift below the yield stress to also be common. Prefactors may change so that in other classes of YSF the strain shifts may be smaller than $(\sigma_y/\sigma_0)\gamma_0$, but we still expect that they will exist.

By looking at the strain shift under stress-controlled oscillatory shear, we can determine when and how materials flow. This has wide reaching applications beyond yield stress fluids. In the derivation of Eq. (39), which relates the strain shift to the fluid component of the dynamic loss modulus, there are no assumptions about the material being a yield stress fluid. Therefore, this experiment and expression can be applied to study flow in any variety of systems under stress-controlled oscillatory shear.

By performing the strain shift experiment and using the relations derived in this work, we have shown that it is possible to gain access to more information than traditional oscillatory testing and analysis alone. This information is freely available in the material response, making it an attractive protocol for any study. Furthermore, because we now understand the physics behind the strain shift, we can accurately use any phase angle to acquire more information than previously achievable. Given the detailed information available from stress-controlled oscillatory shear tests with strain shift, we believe that this protocol should become the standard for rheological oscillatory testing moving forward.

ACKNOWLEDGMENTS

This material is based upon work supported by NSF Grant No. 1847389 and the Laboratory Directed Research and Development program at Sandia National Laboratories. Sandia National Laboratories is a multimission laboratory managed and operated by National Technology and Engineering Solutions of Sandia LLC, a wholly owned subsidiary of Honeywell International Inc., for the US Department of Energy's National Nuclear Security Administration Contract No. DE-NA0003525.

AUTHOR DECLARATIONS

Conflict of Interest

The authors have no conflicts to disclose.

DATA AVAILABILITY

The data that support the findings of this study are available from the corresponding author upon reasonable request.

REFERENCES

[1] Joyner, H. S., "Nonlinear (large-amplitude oscillatory shear) rheological properties and their impact on food processing and quality," Annu. Rev. Food Sci. Technol. **12**, 591–609 (2021).

[2] Ozkan, S., T. W. Gillece, L. Senak, and D. J. Moore, "Characterization of yield stress and slip behaviour of skin/hair care gels using steady flow and LAOS measurements and their correlation with sensorial attributes," Int. J. Cosmet. Sci. **34**, 193–201 (2012).

[3] Ducoulombier, N., R. Mesnil, P. Carneau, L. Demont, H. Bessaies-Bey, J.-F. Caron, and N. Roussel, "The 'Slugs-test' for extrusion-based additive manufacturing: Protocol, analysis and practical limits," Cem. Concr. Compos. **121**, 104074 (2021).

[4] Banfill, P. F. G., "Rheology of fresh cement and concrete," in *Rheology Reviews 2006* (British Society of Rheology, 2006), pp. 61–130.

[5] Qazi, T. H., V. G. Muir, and J. A. Burdick, "Methods to characterize granular hydrogel rheological properties, porosity, and cell invasion," ACS Biomater. Sci. Eng. **8**, 1427–1442 (2022).

[6] Kostynick, R., H. Matinpour, S. Pradeep, S. Haber, A. Sauret, E. Meiburg, T. Dunne, P. Arratia, and D. Jerolmack, "Rheology of debris flow materials is controlled by the distance from jamming," Proc. Natl. Acad. Sci. U.S.A. **119**, e2209109119 (2022).

[7] Coussot, P., and J. M. Piau, "On the behavior of fine mud suspensions," Rheol. Acta **33**, 175–184 (1994).

[8] Chang, C., and P. A. Smith, "Rheological characterization of nuclear waste slurries," Part. Sci. Technol. **14**, 165–180 (1996).

[9] Balmforth, N. J., A. S. Burbidge, R. V. Craster, J. Salzig, and A. Shen, "Visco-plastic models of isothermal lava domes," J. Fluid Mech. **403**, 37–65 (2000).

[10] Oldroyd, J. G., "A rational formulation of the equations of plastic flow for a Bingham solid," Math. Proc. Cambridge Philos. Soc. **43**, 100–105 (1947).

[11] Hohenemser, K., and W. Prager, "Über die ansätze der mechanik isotroper kontinua," Z. Angew. Math. Mech. **12**, 216–226 (1932).

[12] Prager, W., *Introduction to Mechanics of Continua* (Dover Publications, Mineola, NY, 1961).

[13] Nguyen, Q. D., and D. V. Boger, "Measuring the flow properties of yield stress fluids," Annu. Rev. Fluid Mech. **24**, 47–88 (1992).

[14] Frigaard, I., "Simple yield stress fluids," Curr. Opin. Colloid Interface Sci. Rheol. **43**, 80–93 (2019).

[15] Saramito, P., "A new constitutive equation for elastoviscoplastic fluid flows," J. Non-Newtonian Fluid Mech. **145**, 1–14 (2007).

[16] Bonn, D., and M. M. Denn, "Yield stress fluids slowly yield to analysis," Science **324**, 1401–1402 (2009).

[17] Reiner, M., "Rheology," in *Elasticity and Plasticity* (Springer Berlin, Heidelberg, Germany, 1958), pp. 434–550.

[18] Weissenberg, K., "A continuum theory of rheological phenomena," Nature **159**, 310–311 (1947).

[19] Donley, G. J., P. K. Singh, A. Shetty, and S. A. Rogers, "Elucidating the G″ overshoot in soft materials with a yield transition via a time-resolved experimental strain decomposition," Proc. Natl. Acad. Sci. U.S.A. **117**, 21945–21952 (2020).

[20] Kamani, K., G. J. Donley, and S. A. Rogers, "Unification of the rheological physics of yield stress fluids," Phys. Rev. Lett. **126**, 218002 (2021).

[21] Kamani, K. M., G. J. Donley, R. Rao, A. M. Grillet, C. Roberts, A. Shetty, and S. A. Rogers, "Understanding the transient large amplitude oscillatory shear behavior of yield stress fluids," J. Rheol. **67**, 331–352 (2023).

[22] Dinkgreve, M., J. Paredes, M. M. Denn, and D. Bonn, "On different ways of measuring 'the' yield stress," J. Non-Newtonian Fluid Mech. **238**, 233–241 (2016).

[23] Bingham, E. C., *Fluidity and Plasticity* (McGraw-Hill Book Company, Inc., New York, 1922).

[24] Herschel, W. H., and R. Bulkley, "Measurement of consistency as applied to rubber-benzene solutions," Proc. Am. Soc. Test. Mater. **26**, 621–633 (1926).

[25] Casson, N., *A Flow Equation for Pigment-oil Suspensions of the Printing Ink Type*, Reprinted from "Rheology of Disperse Systems." (Pergamon Press, Oxford, UK, 1959).

[26] Barnes, H. A., and K. Walters, "The yield stress myth?," Rheol. Acta **24**, 323–326 (1985).

[27] Astarita, G., "Letter to the editor: The engineering reality of the yield stress," J. Rheol. **34**, 275–277 (1990).

[28] Barnes, H. A., "The yield stress—a review or '$\pi\alpha\nu\tau\alpha\ \rho\epsilon\ell$'—everything flows?," J. Non-Newtonian Fluid Mech. **81**, 133–178 (1999).

[29] Laurati, M., S. U. Egelhaaf, and G. Petekidis, "Plastic rearrangements in colloidal gels investigated by LAOS and LS-Echo," J. Rheol. **58**, 1395–1417 (2014).

[30] Masalova, I., A. Y. Malkin, and R. Foudazi, "Yield stress as measured in steady shearing and in oscillations" Appl. Rheol. **18**, 44790 (2008).

[31] Tschoegl, N. W., "Energy storage and dissipation in a linear viscoelastic material," in *The Phenomenological Theory of Linear Viscoelastic Behavior: An Introduction* (Springer Berlin, Heidelberg, Germany, 1989), pp. 443–488.

[32] Shih, W. Y., W.-H. Shih, and I. A. Aksay, "Elastic and yield behavior of strongly flocculated colloids," J. Am. Ceram. Soc. **82**, 616–624 (1999).

[33] Rouyer, F., S. Cohen-Addad, and R. Höhler, "Is the yield stress of aqueous foam a well-defined quantity?," Colloids Surf., A **263**, 111–116 (2005).

[34] Mason, T. G., J. Bibette, and D. A. Weitz, "Yielding and flow of monodisperse emulsions," J. Colloid Interface Sci. **179**, 439–448 (1996).

[35] Mezger, T. G., *The Rheology Handbook: For Users of Rotational and Oscillatory Rheometers* (Vincentz Network, Hannover, Germany, 2006).

[36] Walls, H. J., S. B. Caines, A. M. Sanchez, and S. A. Khan, "Yield stress and wall slip phenomena in colloidal silica gels," J. Rheol. **47**, 847–868 (2003).

[37] Hyun, K., S. H. Kim, K. H. Ahn, and S. J. Lee, "Large amplitude oscillatory shear as a way to classify the complex fluids," J. Non-Newtonian Fluid Mech. **107**, 51–65 (2002).

[38] Isayev, A. I., and X. Fan, "Viscoelastic plastic constitutive equation for flow of particle filled polymers," J. Rheol. **34**, 35–54 (1990).

[39] Houlsby, G. T., and A. M. Puzrin, "Rate-dependent plasticity models derived from potential functions," J. Rheol. **46**, 113–126 (2002).

[40] Saramito, P., "A new elastoviscoplastic model based on the Herschel-Bulkley viscoplastic model," J. Non-Newtonian Fluid Mech. **158**, 154–161 (2009).

[41] Lee, J. C.-W., Y.-T. Hong, K. M. Weigandt, E. G. Kelley, H. Kong, and S. A. Rogers, "Strain shifts under stress-controlled oscillatory shearing in theoretical, experimental, and structural perspectives: Application to probing zero-shear viscosity," J. Rheol. **63**, 863–881 (2019).

[42] Hassager, O., "Stress-controlled oscillatory flow initiated at time zero: A linear viscoelastic analysis," J. Rheol. **64**, 545–550 (2020).

[43] Ogunkeye, A., R. E. Hudson, and D. J. Curtis, "The effect of instrument inertia on the initiation of oscillatory flow in stress controlled rheometry," J. Rheol. **67**, 1175–1187 (2023).

[44] Ewoldt, R. H., "Defining nonlinear rheological material functions for oscillatory shear," J. Rheol. **57**, 177–195 (2013).

[45] Dimitriou, C. J., R. H. Ewoldt, and G. H. McKinley, "Describing and prescribing the constitutive response of yield stress fluids using large amplitude oscillatory shear stress (LAOStress)," J. Rheol. **57**, 27–70 (2013).

[46] Pipkin, A. C., *Lectures on Viscoelasticity Theory*, Applied Mathematical Sciences, Vol. 7 (Springer, New York, 1986).
[47] Korculanin, O., D. Hermida-Merino, H. Hirsemann, B. Struth, S. A. Rogers, and M. P. Lettinga, "Anomalous structural response of nematic colloidal platelets subjected to large amplitude stress oscillations," Phys. Fluids **29**, 023102 (2017).
[48] Shan, L., H. He, N. J. Wagner, and Z. Li, "Nonlinear rheological behavior of bitumen under LAOS stress," J. Rheol. **62**, 975–989 (2018).
[49] Hwang, D. C., "Rheological characterization and modeling of laponite gels with application to snug-like locomotion," Master's thesis, Massachusetts Institute of Technology, Cambridge, MA, 2005.
[50] Li, J.-J., X. Cheng, Y. Zhang, and W.-X. Sun, "A revisit of strain-rate frequency superposition of dense colloidal suspensions under oscillatory shears," J. Cent. South Univ. **23**, 1873–1882 (2016).
[51] Renardy, M., and T. Wang, "Large amplitude oscillatory shear flows for a model of a thixotropic yield stress fluid," J. Non-Newtonian Fluid Mech. **222**, 1–17 (2015).
[52] Erwin, B. M., M. Cloitre, M. Gauthier, and D. Vlassopoulos, "Dynamics and rheology of colloidal star polymers," Soft Matter **6**, 2825–2833 (2010).
[53] Møller, P. C. F., A. Fall, and D. Bonn, "Origin of apparent viscosity in yield stress fluids below yielding," Europhys. Lett. **87**, 38004–38010 (2009).
[54] Dinkgreve, M., M. M. Denn, and D. Bonn, "'Everything flows?': Elastic effects on startup flows of yield-stress fluids," Rheol. Acta **56**, 189–194 (2017).
[55] Lodge, T. P., and P. C. Hiemenz, *Polymer Chemistry*, 2nd ed. (CRC Press, Boca Raton, FL, 2007).
[56] Mewis, J., and N. J. Wagner, *Colloidal Suspension Rheology*, Cambridge Series in Chemical Engineering (Cambridge University Press, Cambridge, UK, 2011).
[57] Denn, M. M., and D. Bonn, "Issues in the flow of yield-stress liquids," Rheol. Acta **50**, 307–315 (2011).
[58] See the supplementary material online for the following. Section A contains a graphical representation and further descriptions of the experimental protocol. Section B contains a discussion on the strain resolution of the rheometer, and its relation to the strain shift. Section C contains a derivation of the KDR for a creep test, to support our assertion that yield stress fluids will demonstrate finite flow below the yield stress over finite timescales even for creep tests. Section D contains derivations to help readers to perform the discreet Fourier transform (DFT) for these experiments. We also perform derivations of the compliances and moduli in terms of the results of the DFT. Finally, Sec. E contains additional data including characterizations of 1.8% and 2.0% Carbopol, and the comparisons between iterative recovery rheology to the results of the strain shift experiment for the additional concentrations, as well as additional frequency.